11B.4 INTERANNUAL AND INTERDECADAL VARIATIONS OF TROPICAL CYCLONE ACTIVITY IN THE SOUTH CHINA SEA

Andy Zung-Ching GOH and Johnny C. L. CHAN*

Department of Physics and Materials Sciences, City University of Hong Kong, Hong Kong, China

1. INTRODUCTION

Tropical cyclones (TCs) are one of the deadliest and costliest natural disasters, especially those who live near the coastal areas. TC behaviour in the South China Sea (SCS), however, has been a relatively less studied area.

Past research has shown that TC activity in the WNP exhibit interannual (e.g. Chan 1985) and interdecadal (e.g. Chan and Shi 1996) variations, while El Niño-Southern Oscillation (ENSO) (e.g. Chan 1985) and Pacific Decadal Oscillation (PDO) (e.g. Leung et al. 2005) have been attributed to causing variations in TC activity in the WNP.

Based on Gray's (1968, 1979) six points related to TC genesis and development, seven possible factors are identified to study the effects the large scale atmospheric phenomena of ENSO and PDO have on TC behaviour in the SCS: 850-hPa vorticity, 200-hPa divergence, 850-hPa geopotential height, 200-850-hPa shear, moist static energy (MSE) are the genesis factors, while 500-hPa zonal wind and 500-hPa geopotential height are the steering factors.

It has long been known that ENSO plays a role in shaping the climate in East Asia. It not only affects the formation location and subsequent motions of TCs in WNP (e.g. Chan 2000; Wang and Chan 2002; Chan 2005) and SCS (Liu and Chan 2003), but also the number of TCs in both basins (Li 1988) and that making landfall in southern China (Wu et al. 2004). On the other hand, Liu and Chan (2003) found that TC movement is affected by ENSO, and Leung et al. (2006) further suggested that TC activity in the SCS are modulated by PDO. As some studies (e.g. Hare and Mantua 2000) have pointed out the climatic and biological impacts of the PDO phase around 1976, it is conceivable that this phenomenon is also a factor affecting TC behaviour.

*Corresponding author: Johnny C. L. CHAN Department of Physics and Materials Sciences, City University of Hong Kong, Tat Chee Avenue, Kowloon, Hong Kong, China. Email: johnny.chan@cityu.edu.hk

2. DATA

TC data from the Hong Kong Observatory and atmospheric data from the National Centers for Environmental Prediction–National Center for Atmospheric Research (NCEP-NCAR) Reanalysis Project (Kalnay et al. 1996) after 1965 are utilized in this study. ENSO data are from the Climate Prediction Center of the US National Weather Service (http://www.cpc.ncep.noaa.gov/products/analysis_monitoring/ensostuff/ensoyears.shtml), while PDO data are from the University of Washington's Joint Institute for the Study of the Atmosphere and Ocean (http://jisao.washington.edu/pdo/PDO.latest)

Only TCs that had attained at least tropical storm strength (maximum wind speed > 65 km h^{-1}) are included. TCs in the SCS are divided into those that are formed within the SCS (FORM) and those entering SCS from the WNP (ENT), and the TC season in SCS is divided into May to August (early season) and September to December (late season).

Furthermore, an ENSO index is defined according to Trenberth (1997). An EN (a LN) event lasts for as long as this index exceeds the +(-) 0.4°C

threshold, and an EN (a LN) year is defined as the onset year of the event. According to this, 12 EN events and 10 LN events are found in the 41 years from 1965 to 2005. On the other hand, using Mantua's (1999) definition of the PDO index, a year is designated PDO positive (negative) if the index is greater (less) than zero. In total, there are 23 PDO+ and 18 PDO- events between 1965 and 2005.

3. INTERANNUAL AND INTERDECADAL VARIATIONS IN TC ACTIVITY

3.1 *Trend analysis*

There is a statistically significant decreasing trend in the total number of TCs (N_T) and number of ENT (N_E), and an insignificant trend in the number of FORM (N_F) in the whole (Fig. 1), early (Fig. 2), and late (Fig. 3) seasons over the study period.

3.2 *Periodicity of TC occurrences*

Using a Mexican-hat wavelet (Derivative of Gaussian with m=2) as the basis function, wavelet analysis is employed to determine the periodicity of TC occurrences in the basin. The domain for this analysis is 0° to 45°N, 100°E to 160°E, as this is where most TCs the WNP are found. Periodicity for N_E and N_F in all seasons are shown in Fig. 4.

A change in periodicity can be seen around 1976 or 77 for N_E and N_F in the whole and late seasons and N_F in the early season. Before the shift, a shorter periodicity can be seen in both the N_E and N_F series (2 to 6 years and 5 to 8 years respectively). This short periodicity is resumed between 1990 and 2003 in the N_E series, but is not found in the N_F series. This change in periodicity in the mid 70s can be seen in the early and late seasons, as the early season N_F shifted from a periodicity of 4 to 8 years to that of 2 to 8 years between 1990 and 2003, and the late season N_E shifted from a 2 to 6 year period to one more than 16 years. Similarly, there is a periodicity of 8 to 20 years in the late season N_F (Fig. 4f) before 1980, which decreases to 4 to 8 years in the 1980s. After that, no periodicity can be seen until between 1995 and 2000 when a period of 2 to 8 years is found.

Thus, it is apparent from these results that TC activity in the SCS has a decreasing trend and possesses significant interannual and interdecadal variabilities. The shorter periodicities coincide with the 3- to 7- year period of ENSO, suggesting that ENSO maybe a factor affecting TCs in the SCS. However, as there are only 41 years of data, longer periods cannot be identified. Nonetheless, the periodicities that are over 16 years might be related to the PDO, as its period can range from 20 to 30 years.

3.3 *TC behaviour during different phases of ENSO and PDO*

A comparison of the number of years with above- or below-normal TC activity shows that TC behaviour during EN and LN are mostly opposite, with EN favouring below-normal activities for TOT and ENT (Table 1). However, the situation for FORM is similar in EN and LN. This suggests that the effect of ENSO is less on TCs formed in the SCS. Similarly, below-normal TC activities are favoured during PDO+, while the opposite is true during PDO- (Table 2). These results suggest that the effects of ENSO and PDO are more prominent in the late season, which is reasonable as this is the time when these two phenomena peak.

4 FACTORS AFFECTING TC BEHAVIOUR IN DIFFERENT PHASES OF ENSO AND PDO

Empirical Orthogonal Function (EOF) analysis is employed to the seven factors discussed in Section 1 are to investigate the reason for the observed differences in TC behaviour between the two phases

of ENSO and PDO. The eight factor EOFs that contributes the most to explaining the observed TC behaviour under the different scenarios are determined the seven factors discussed in Section 1 are by a stepwise regression analysis. Limiting the number of factors chosen to eight is to avoid having a large number of factors chosen, so as to minimize the risk that some of the chosen factors are not independent from each other (Paeth et al. 2006). North et al. (1982)'s method is used to estimate the sampling errors in EOFs. In the following, the last number in the abbreviations of the factors indicates the EOF, 1 for the first EOF, 2 for the second etc. Only the late season is considered, as this is when both ENSO and PDO have the largest effect.

4.1 *FORM in the late season*

The linear regression equation is given by

$$\begin{aligned}\mathrm{FORM_l} &= 0.019 + 0.315\times 500\mathrm{U}_1 - 0.387\times 500\mathrm{U}_2 \\ &- 0.047\times \mathrm{DIV}_1 - 0.188\times \mathrm{DIV}_2 - 0.287\times \mathrm{DIV}_3 \\ &+ 0.193\times \mathrm{MSE}_1 + 0.366\times \mathrm{MSE}_2 - 0.130\times \mathrm{SHR}_3\end{aligned}$$

This regression equation gives a multiple correlation coefficient of 0.955, which is 95% significant.

4.1.1 *ENSO*

In general, the situation in EN and LN are quite similar when FORM is considered (Fig. 5). Apart from 500U1 and MSE1, both of which indicate that the situation in EN (Figs. 5a and 5f) is not as advantageous to TC genesis as that in LN (Figs. 6a and 6f), others seem to point out that the major difference between TC behaviour in EN and LN is the location of formation, with less indication on the difference in number. For example, DIV2 (Figs. 5d and 6d), DIV3 (Figs. 5e and 6e), and MSE2 (Figs. 5g and 6g) all indicate favourable situation for TC formation inside the SCS during both phases of ENSO. However, the pattern of DIV3 seems to point out that more TCs form in the northern (southern) part of the SCS during EN (LN). This is supported by the flow pattern at the 500-hPa level. In northern SCS, although the pattern of 500U2 effectively forms an anticyclonic anomaly during both EN (Fig. 5b) and LN (Fig. 6b), indicating less deep convection in the area, the magnitude of this factor EOF is quite small. On the other hand, the pattern of 500U1 in southern SCS reveals a cyclonic (an anticyclonic) anomaly centred over 10°N during LN (EN). Thus, in the north, the larger DIV2 means more FORM in this part of SCS during EN. In the south, the cyclone (anticyclone) at 500-hPa enhances (suppresses) deep convection, and is advantageous (disadvantageous) to the genesis of TCs, and infers more (less) FORM during LN (EN). Considering the effects of DIV2, DIV3, 500U1, and 500U2, it can be concluded that TCs in EN (LN) would preferably form in northern (southern) SCS. This is in fact the case, with the average formation latitude of TCs during EN being 14.8°N, while it is 12.6°N during LN, and this difference is statistically significant at the 95% confidence level. This north-south discrepancy is not seen in the WNP in the late season, and is opposite to the situation in the early season, where TCs in LN are found to form preferably to the north, while those in EN to south (Chen et al. 1998).

Various studies have pointed out the relationship between the TC formation location and the monsoon trough in the WNP (e.g. Lander 1994, Chen et al. 1998). Analysis of the 850-hPa flow pattern in the late season (not shown) reveals that the monsoon trough is nearly non-existent inside the SCS during EN, whereas it is located along around 8°N during LN. Outside of the SCS, in the WNP, the eastern tail of the monsoon trough extends along about the same latitude during both phases of ENSO. Thus, the absence of the monsoon trough inside the

SCS is able to explain the lack of FORM during EN, and that the monsoon trough lies along the same latitude in the WNP during both EN and LN can account for the lack of north-south discrepancy in TC number in WNP.

4.1.2 *PDO*

Although observations suggest more FORM during PDO-, the factor EOFs seem to give inconclusive results. This could be the reason for the difference between FORM during PDO+ and PDO- being only statistically significant at 90%. Nonetheless, in general, the flow patterns during PDO- seem to be in agreement with the observation that TC formation inside the SCS is favoured during this phase of the PDO, with DIV1 (Fig. 8c) and MSE2 (Fig. 8g) being the exception. The situation of DIV1 seems to be explainable if the pattern at the 500-hPa level is considered. The patterns of 500U1 (Fig. 7a) and 500U2 (Fig. 7b) indicate the presence of strong anticyclonic anomalies caused by the strong zonal winds anomalies in both the northern and southern parts of the SCS during PDO+. Considering the strength of this anticyclone, it is possible that its effect could reach into the upper-level, making the circulation anticyclonic. The positive anomaly of divergence can also be seen in DIV2 (Fig. 7d) and DIV3 (Fig. 7e), albeit only over the southern part of SCS, possibly due to the same reason. As for the pattern in MSE2, although it suggests that TC formation is favoured over the northern SCS, its effect might be overcome by those of the other factors that indicate the situation is unsuitable for TC genesis in northern SCS. This also shows that even if the thermodynamic conditions are suitable for cyclogenesis, if the dynamical conditions are not, TCs formation would still be inhibited.

4.2 *ENT in the late season*

The linear regression equation is given by

$$\begin{aligned}\mathrm{ENT_I} &= -0.098 + 1.422 \times 500\mathrm{U}_1 + 0.179 \times \mathrm{DIV}_3 \\ &+ 1.333 \times \mathrm{HGT}_1 - 0.539 \times \mathrm{HGT}_2 - 0.448 \times \mathrm{HGT}_3 \\ &+ 0.349 \times \mathrm{MSE}_3 - 0.575 \times \mathrm{VOR}_1 + 0.301 \times \mathrm{VOR}_2\end{aligned}$$

This regression equation gives a multiple correlation coefficient of 0.956, which is significant at the 95% confidence leve.

4.2.1 *ENSO*

Figure 7 shows the behaviour of the factor EOFs affecting ENT during EN and LN. Recall that ENT in the late season is less during EN and more during LN. Indeed, the genesis factors indicate that in general, less TCs are formed in the EOF analysis domain over the WNP during EN. This could be due to the case that TCs tend to form more towards the east and the south during EN, which causes the EOF analysis to indicate below-normal formation near the Philippines. At the same time, all the steering factors, except 500H1 (Fig. 9b), suggest that the situation during EN does not favour TCs being steered into the SCS. Specifically, the patterns of 500H2 (Fig. 9c) and 500H3 (Fig. 9d) show a southeasterly to southerly flow around 130°E. Considering the formation location of TCs during EN, it is possible that those TCs are caught in this flow, causing them to recurve. On the other hand, although there is no conclusive evidence that more TCs are steered into the SCS during LN, the genesis factors indicate that more TCs are formed in the WNP, which may explain the higher ENT during this phase of ENSO. It can be seen that all the EOFs of 500-hPa geopotential height exhibit above- (below-) normal anomaly during EN (LN). Chan (1985) indicated that during EN, an anomalous Walker circulation would be formed, such that sinking motion could be found in the western WNP. The

anomalous high pressure is the result of this sinking motion, and this subsidence would inhibit TC activities. Various literature also agrees that the anomalous Walker circulation would affect TC genesis location and thus activities (e.g. Chen et al. 1998, Wang and Chan 2002). Thus, this at least partly explains the below normal ENT observed during EN.

4.2.2 PDO

It is obvious that the situation during PDO- is more advantageous to the forming of TCs in the WNP, as revealed by every factor EOF related to formation of TCs. Moreover, the movement-related factor EOF of 500U1 (Fig. 12a) also indicates a preference for the steering of TCs into the SCS during PDO-. It is noteworthy that similar to the situation during EN, the flow at 500-hPa seems to favour recurvature of TCs during PDO+. This could be the result of the forcing of PDO by ENSO, as described by Newman et al. (2003), where a positive (negative) phase of PDO is the result of an EN (a LN) during the previous few seasons. Another point worth noting is the positive height anomaly in 500H2 (Fig. 11c) and 500H3 (Fig. 11d) in the northern WNP during PDO+ as opposed to the negative anomaly during PDO-. The cooler (warmer) than normal SST of the northern WNP during PDO+ (PDO-) could be the reason for this, as the lower (higher) SST causes enhanced subsidence (convection), leading to the development of the anomalous high (low). This difference was also documented by Hartmann and Wendler (2005), and seems to be the cause of the recurvature of TCs during PDO+. The patterns of MSE3 (Figs. 11g and 12g) and VOR1 (Figs. 11h and 12h) both show variations in the signs of the anomaly in different areas of WNP, especially near the active TC genesis areas. Analysis of the average genesis location revealed that TCs during PDO+ tend to form in areas with negative anomalies of both MSE3 and VOR1, while during PDO-, they are more likely to form in areas where these two factor EOFs have positive anomalies. Since there are many factors affecting the formation location of TCs, it is possible that even though there are some factors that imply a certain area to be unfavourable for TC genesis, other factors exist that may have a large enough effect to overcome the negative impact. Both MSE3 and VOR1 in PDO+ fall into this category, as deduced from the average formation location of the TCs during this period. This can also explain the lower ENT during PDO+, as less TCs are formed due to the negative impact of both MSE3 and VOR1.

The effects of PDO on ENT in late season are thus manifested on both the formation and steering of TCs. During PDO+, the situation in WNP is such that cyclogenesis is not favoured or inhibited, and the flow patterns are such that TCs tend to recurve or are prevented from entering the SCS. The situation is opposite during PDO-, where most of the factor EOFs are advantageous for TCs to form in WNP, and the steering flow is such that TCs can be steered into the SCS. Obviously, the different behaviour of the factor EOFs is the reason for the difference in ENT between the two phases of PDO.

5 SUMMARY AND DISCUSSION

This study has shown that TCs are affected by large-scale atmospheric phenomena. TCs in the SCS are either formed in the WNP and subsequently steered into the basin (ENT), or simply formed inside the basin (FORM). Similar to their counterparts in the WNP, SCS TCs also show interannual and interdecadal variations in number. ENT has shown a decreasing trend over the study period in both the early and late seasons, while FORM has not changed significantly over the years.

Wavelet analysis has lent support to the hypothesis that TC activities in the SCS are modulated by ENSO. Specifically, ENT in the whole and late seasons shares the same periodicity with ENSO before 1976, as is FORM in the early season. ENT in the early and late seasons, as well as FORM in the late season also shows longer periodicities, which could be related to PDO. As for TC activity, EN (LN) tends to bring below-(above-) normal ENT and FORM.

The cause for all these differences and trends in ENT and FORM can be traced back to the behaviour of their respective factor EOFs, most of which are affected by ENSO. Analysis of factors affecting ENT indicates that TCs are indeed first formed in the WNP and subsequently steered into the SCS by the 500-hPa flow. Formation of TCs in the WNP has a tendency to cause more TCs to be generated in the WNP during LN. The flow patterns during this situation are also generally easterlies, and thus are favourable for TCs to be steered into the SCS. On the contrary, during EN, formation of TCs inside the WNP is generally inhibited, and the steering flow tends to cause TCs to recurve such that they cannot reach the SCS.

The conditions within the SCS are crucial in determining the behaviour of FORM, as results indicate that TCs formed inside the basin are generally not due to convection from outside being steered into SCS. In general, TC formation is inhibited during EN and more FORM can be seen during LN. An interesting point to note is the north-south discrepancy in TCs formed between EN and LN, which is found to be the result of the difference in the location and strength of the monsoon trough during these two phases of ENSO. Thus, it is obvious that similar to the situation in the WNP, the interannual and interdecadal variations in TC activity inside the SCS are caused by ENSO, which causes variations in the factors affecting TC behaviour.

REFERENCES:

Chan, J. C. -L., 1985: Tropical cyclone activity in the northwest Pacific in relation to the El Niño/Southern Oscillation phenomenon. *Mon. Wea. Rev.,* **113,** 599–606.

Chan, J. C. -L., 2000: Tropical cyclone activity over the Western North Pacific associated with El Niño and La Niña events. *J. Climate*, **13**, 2960–2972.

Chan, J. C. -L., 2005: Interannual and interdecadal variations of tropical cyclone activity over the Western North Pacific. *Meteorology and Atmospheric Physics*, **89**, 143–152.

Chan, J. C. -L. and J. E. Shi, 1996: Long-term trends and interannual variability in tropical cyclone activity over the Western North Pacific. *Geophys. Res. Lett.*, **23**, 2765–2767.

Chen, T. -C., S. -P. Weng, N. Yamazaki, and S. Kiehne, 1998: Interannual variation in the tropical cyclone formation over the Western North Pacific. *Mon. Wea. Rev.*, **126**, 1080–1090.

Gray, W. M., 1968: Global view of the origin of tropical disturbances and storms. *Mon. Wea. Rev.*, **96**, 669–700.

Gray, W. M., 1979: Hurricanes: Their formation, structure and likely role in the tropical circulation. *Meteorology Over Tropical Oceans. D. B. Shaw (Ed.), Roy. Meteor. Soc., James Glaisher House, Grenville Place, Bracknell, Berkshire, RG12 1BX*, 155-218.

Kalnay, E., and Coauthors, 1996: The NCEP/NCAR 40-year reanalysis project. *Bull. Amer. Meteor. Soc.*, **77**, 437–471.

Lander, M. A., 1994: An exploratory analysis of the relationship between tropical storm formation in the Western North Pacific and ENSO. *Mon. Wea. Rev.*, **122**, 6636-6651.

Leung, Y. K., M. C. Wu, and W. L. Chang, 2005: Variations of tropical cyclone activity in the South China Sea. Presented in ESCAP/WMO Typhoon Committee Annual Review 2005, November 2006. *Hong Kong Observatory Reprint No.* **675**.

Li, C., 1988: Actions of typhoons over the western Pacific (including the South China Sea) and El Niño. *Advances in Atmospheric Sciences,* **5,** 107-115.

Liu, K. S. and J. C. -L. Chan, 2003: Climatological characteristics and seasonal forecasting of tropical cyclones making landfall along the South China Coast. *Mon. Wea. Rev.*, **131**, 1650–1662.

Wang, B, and J. C. -L. Chan, 2002: How strong ENSO events affect tropical storm activity over the Western North Pacific. *J. Climate*, **15**, 1643–1658.

Wu, M. C., W. L. Chang and W. M. Leung, 2004: Impacts of El Niño–Southern Oscillation events on tropical cyclone landfalling activity in the Western North Pacific. *J. Climate*, **17**, 1419–1428.

	EN (12 events)			LN (10 events)		
	Whole	Early	Late	Whole	Early	Late
N_T	1/5	2/1	0/5	5/1	3/3	7/0
N_E	3/6	3/4	2/8	4/2	2/3	5/1
N_F	5/4	5/3	2/1	4/1	2/3	5/1

Table 1 TC occurrences in different seasons during EN and LN. x/y represents x years in which TC number is above normal/y years in which TC number is below normal.

	PDO + (23 years)			PDO - (18 years)		
	Whole	Early	Late	Whole	Early	Late
N_T	3/9	3/5	4/8	8/1	9/5	5/0
N_E	5/7	8/6	6/11	7/3	4/5	6/2
N_F	4/9	5/9	3/5	9/2	8/5	7/2

Table 2 Same as Table 1, except for PDO+ and PDO-.

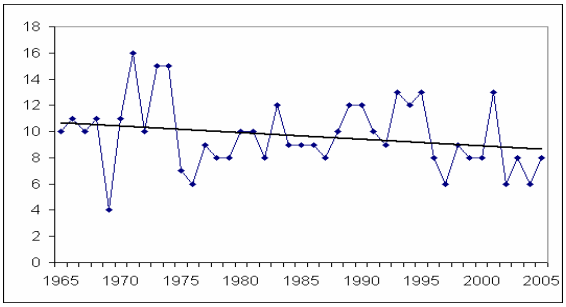

(a)

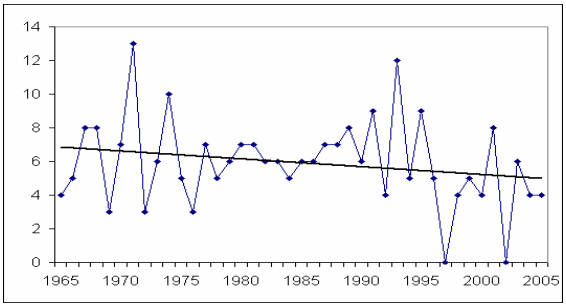

(b)

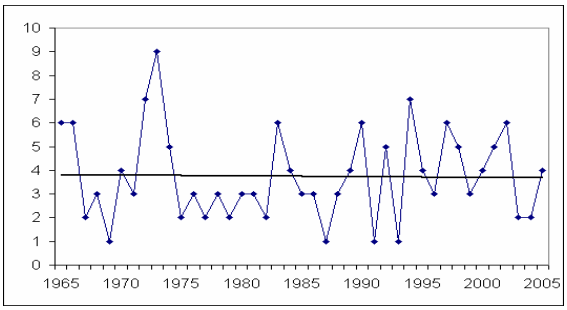

(c)

Figure 1 (a) Total number of TCs (N_T), (b) number of TCs entering (N_E) and (c) number of TCs formed (N_F) in the SCS during the whole season.. The solid straight line indicates the trend.

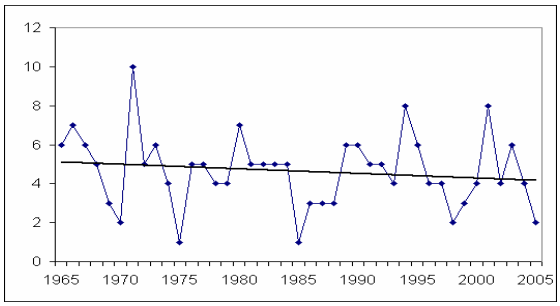

(a)

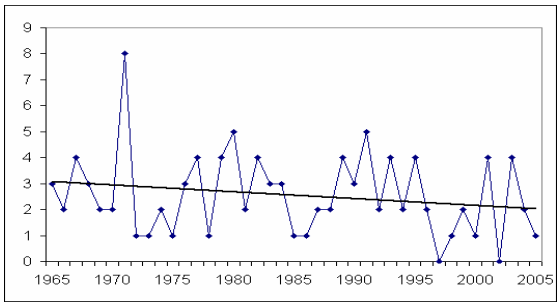

(b)

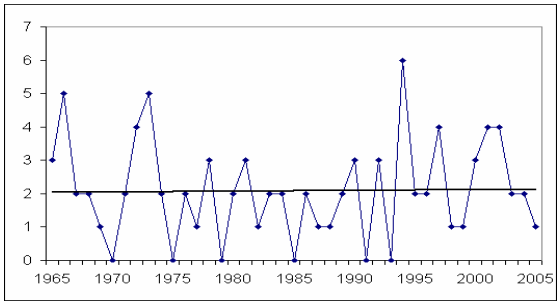

(c)

Figure 2 (a) N_T, (b) N_E, and (c) N_F during the early season. The solid straight line indicates the trend.

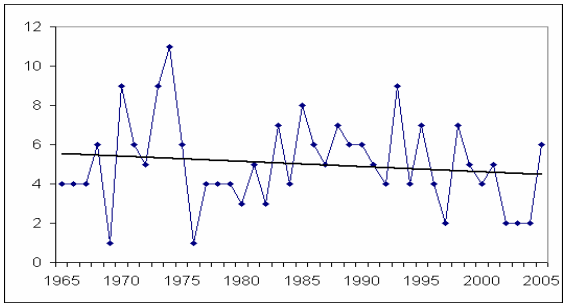

(a)

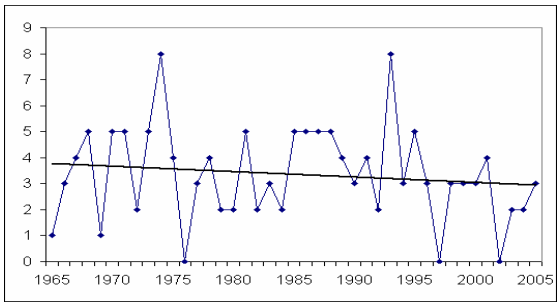

(b)

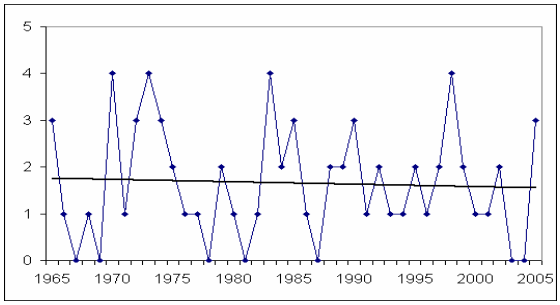

(c)

Figure 3 (a) N_T, (b) N_E, and (c) N_F during the late season. The solid straight line indicates the trend.

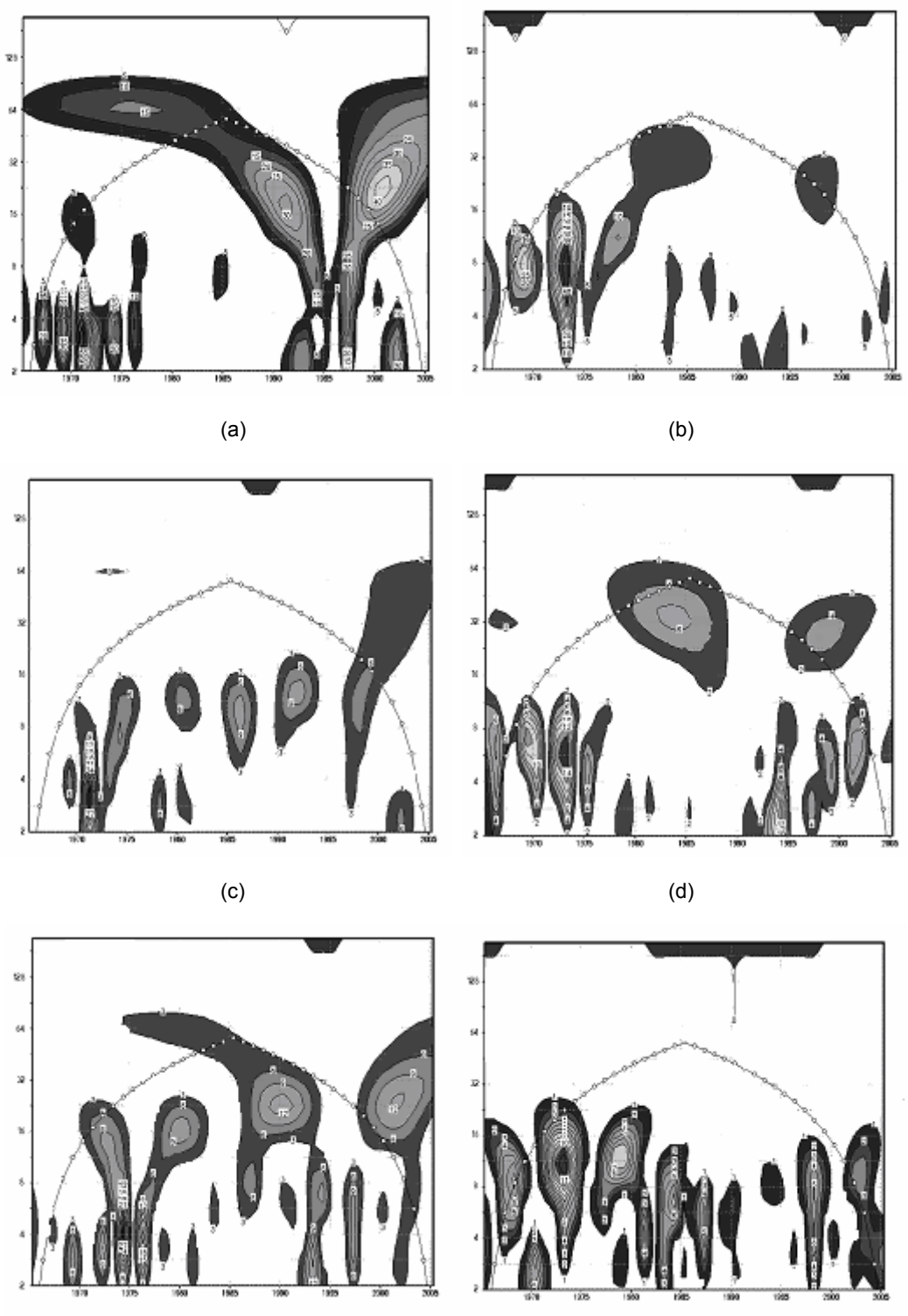

Figure 4 Local wavelet power spectrum for ENT in the (a) whole (c) early and (e) late seasons and in the (b) whole (d) early and (f) late seasons for FORM. Circled line indicates the cone of influence.

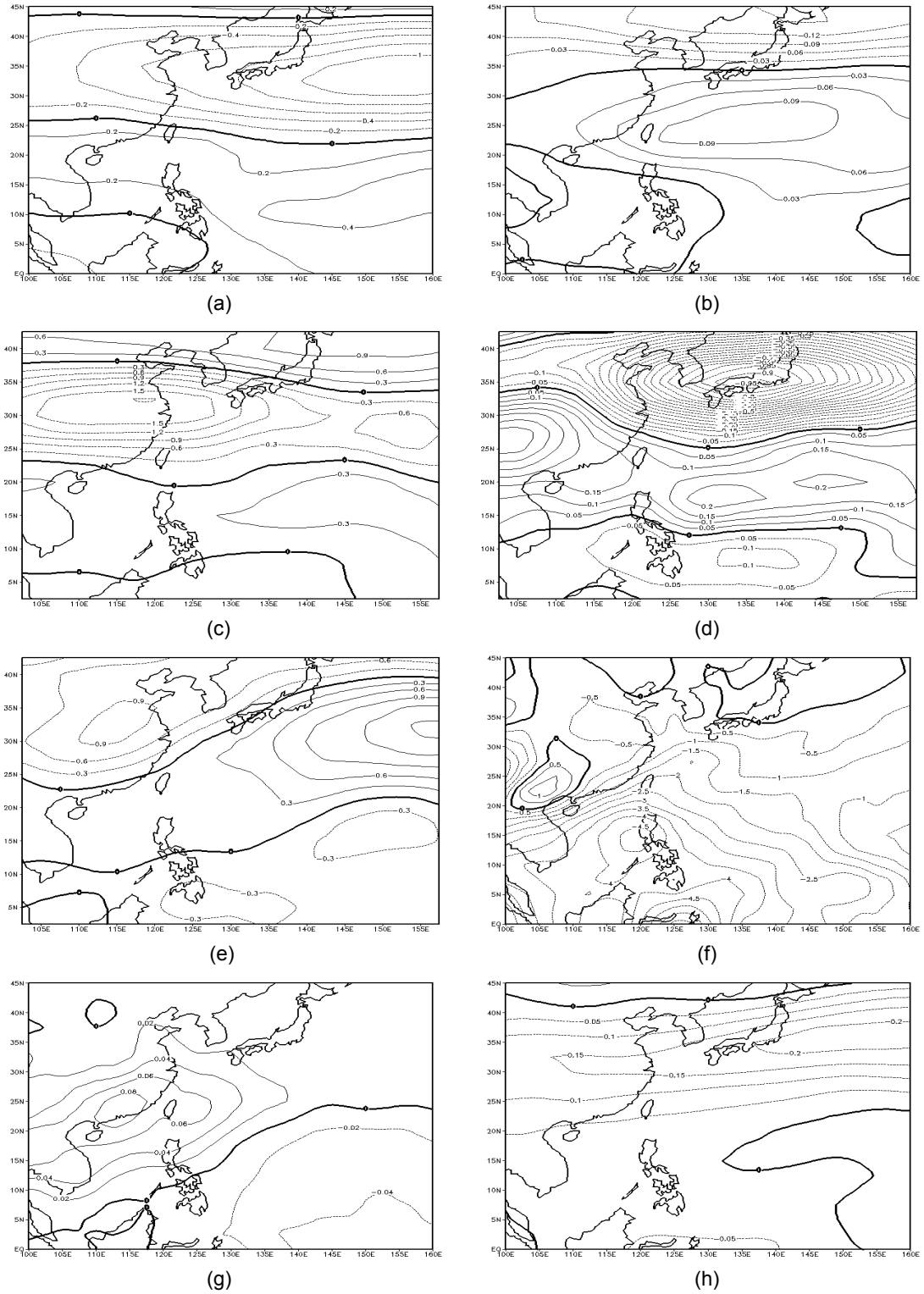

Figure 5 Flow patterns of factor EOFs affecting FORM in the late season during EN. Solid (Dotted) lines indicate positive (negative) anomalies. (a) 500U1 (Unit: ms^{-1}), (b) 500U2 (Unit: ms^{-1}), (c) DIV1 (Unit: $\times 10^{-6}$ s^{-1}), (d) DIV2 (Unit: $\times 10^{-6}$ s^{-1}), (e) DIV3 (Unit: $\times 10^{-6}$ s^{-1}), (f) MSE1 (Unit: $\times 10^{6}$ Wm^{-2}), (g) MSE2 (Unit: $\times 10^{6}$ Wm^{-2}), and (h) SHR3 (Unit: ms^{-1}).

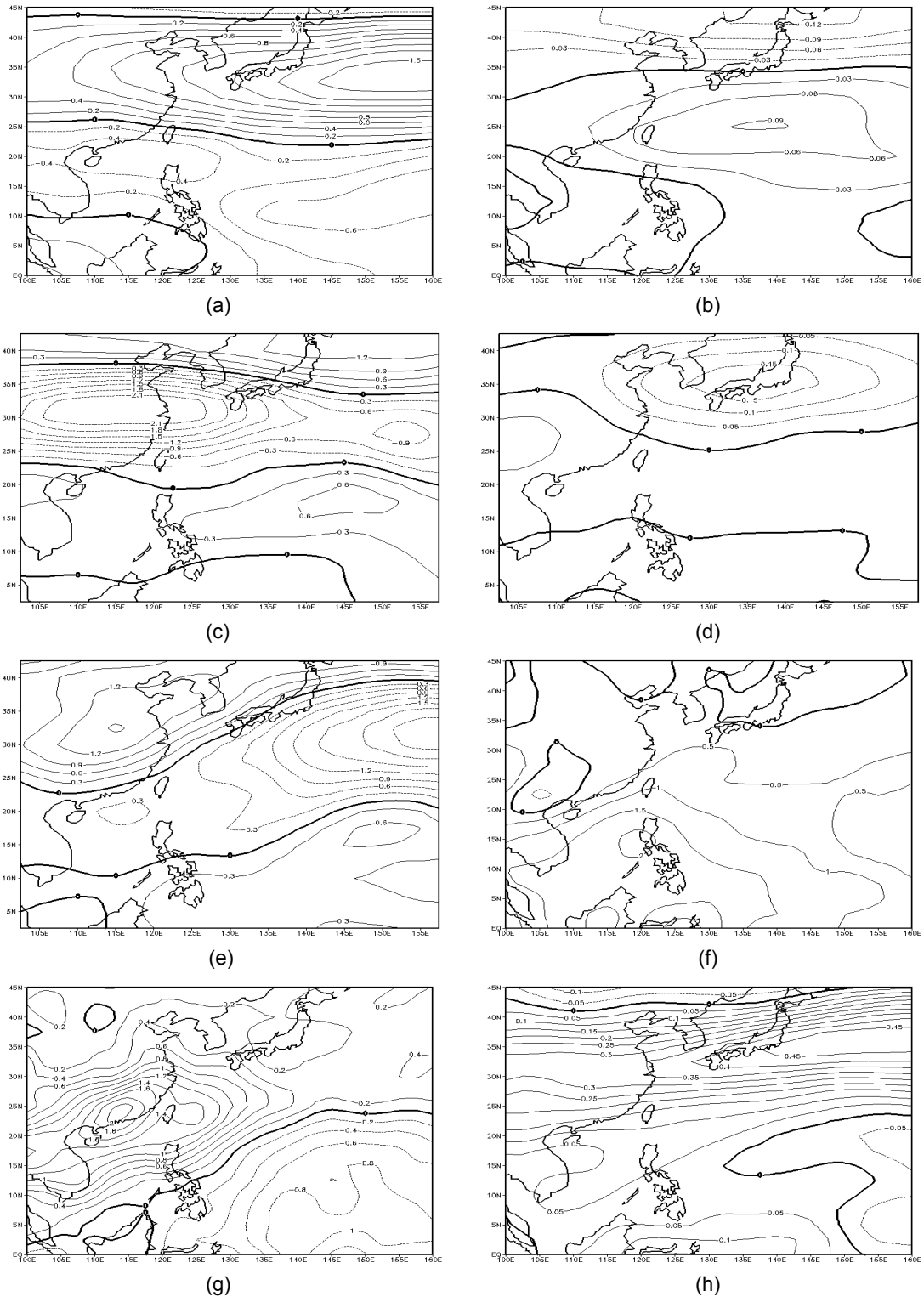

Figure 6 Same as Fig. 5, except for LN.

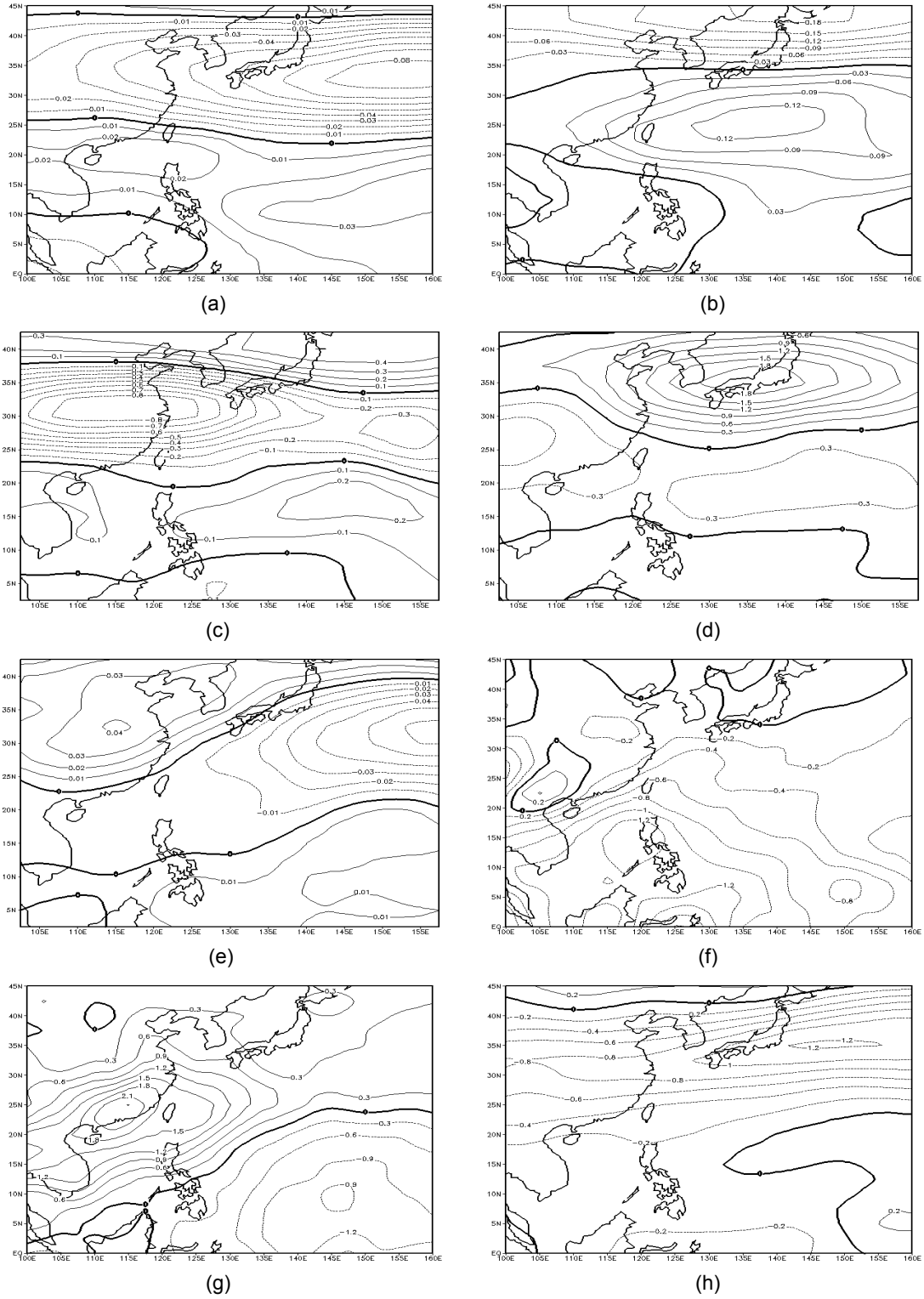

Figure 7 Same as Fig. 5, except for PDO+.

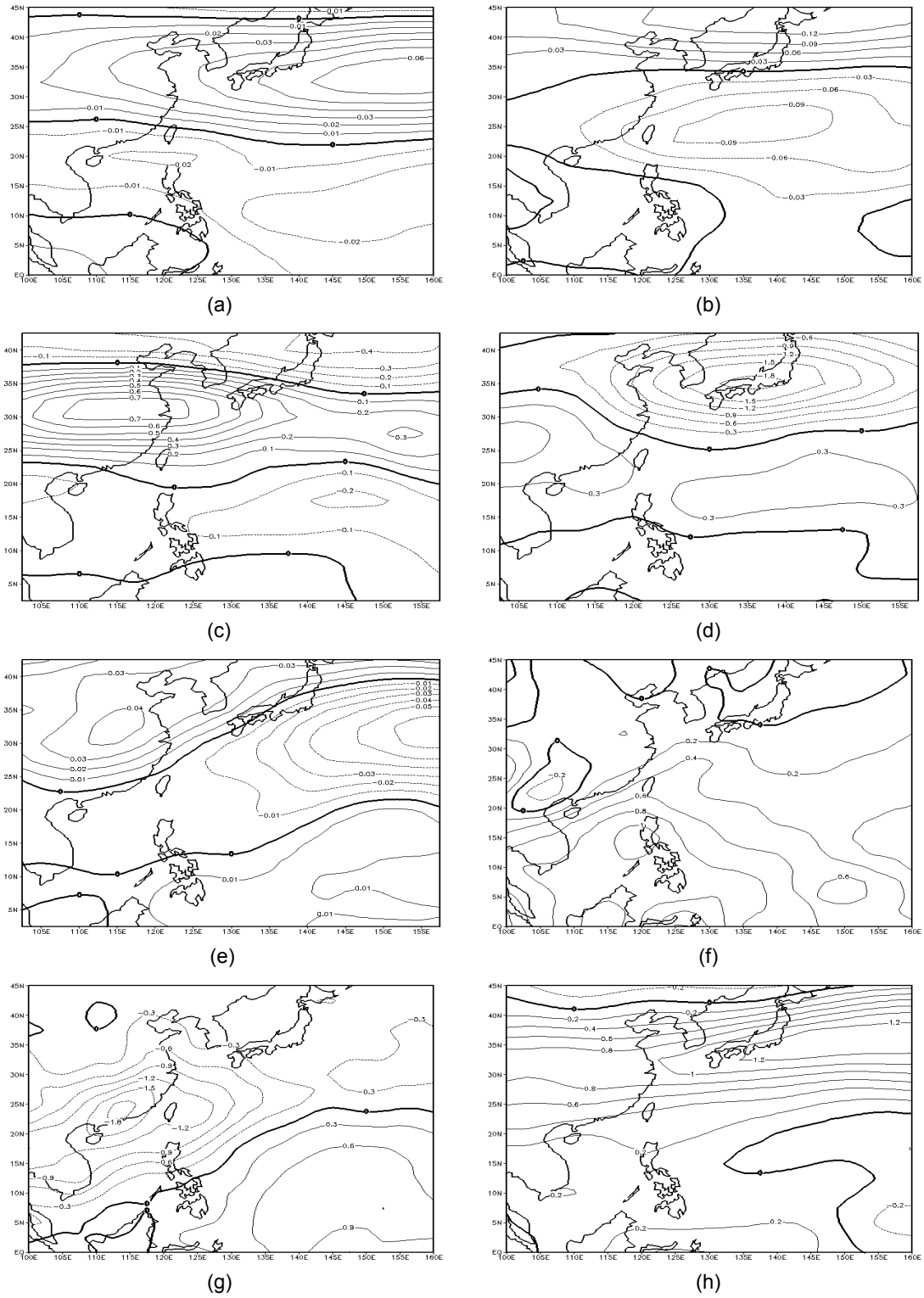

Figure 8 Same as Fig. 5, except for PDO-.

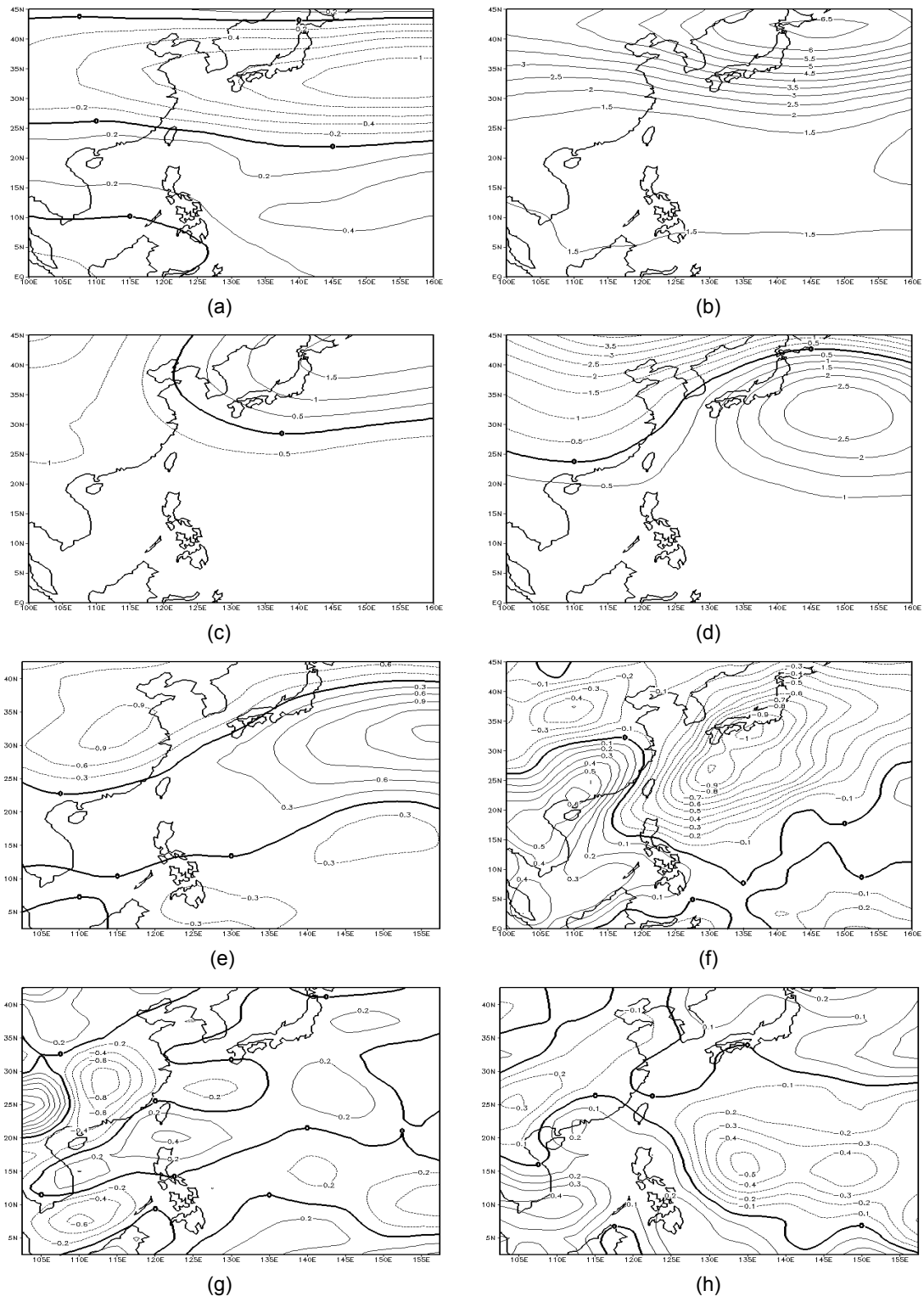

Figure 9 Flow patterns of factor EOFs affecting ENT in the late season during EN. Solid (Dotted) lines indicate positive (negative) anomalies. (a) 500U1 (Unit: ms^{-1}), (b) 500H1 (Unit: gpm), (c) 500H2 (Unit: gpm), (d) 500H3 (Unit: gpm), (e) DIV3 (Unit: $\times 10^{-6}$ s^{-1}), (f) MSE3 (Unit: $\times 10^{6}$ Wm^{-2}), (g) VOR1 (Unit: $\times 10^{-6}$ s^{-1}), and (h) VOR2 (Unit: $\times 10^{-6}$ s^{-1}).

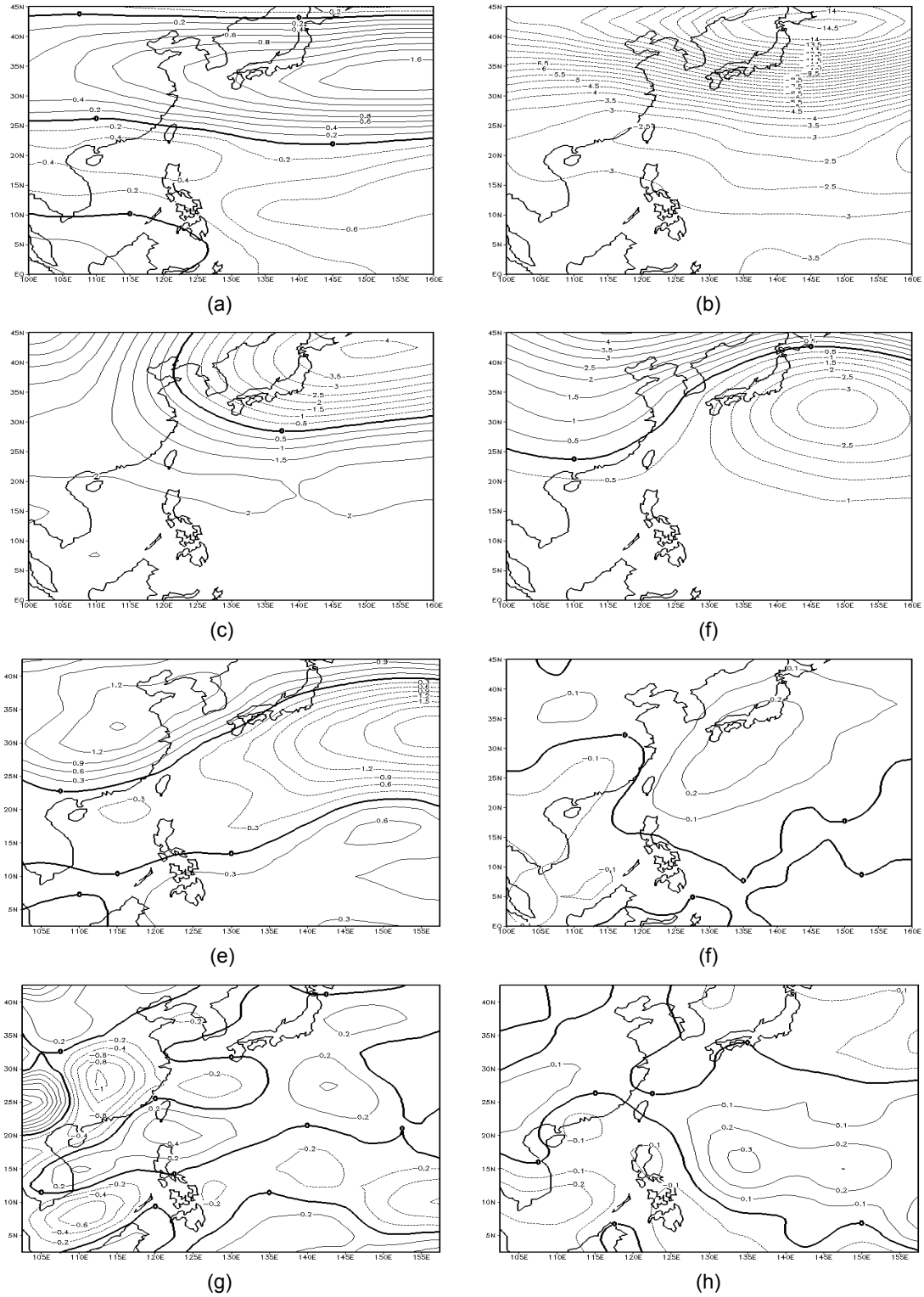

Figure 10 Same as Fig. 9, except for LN.

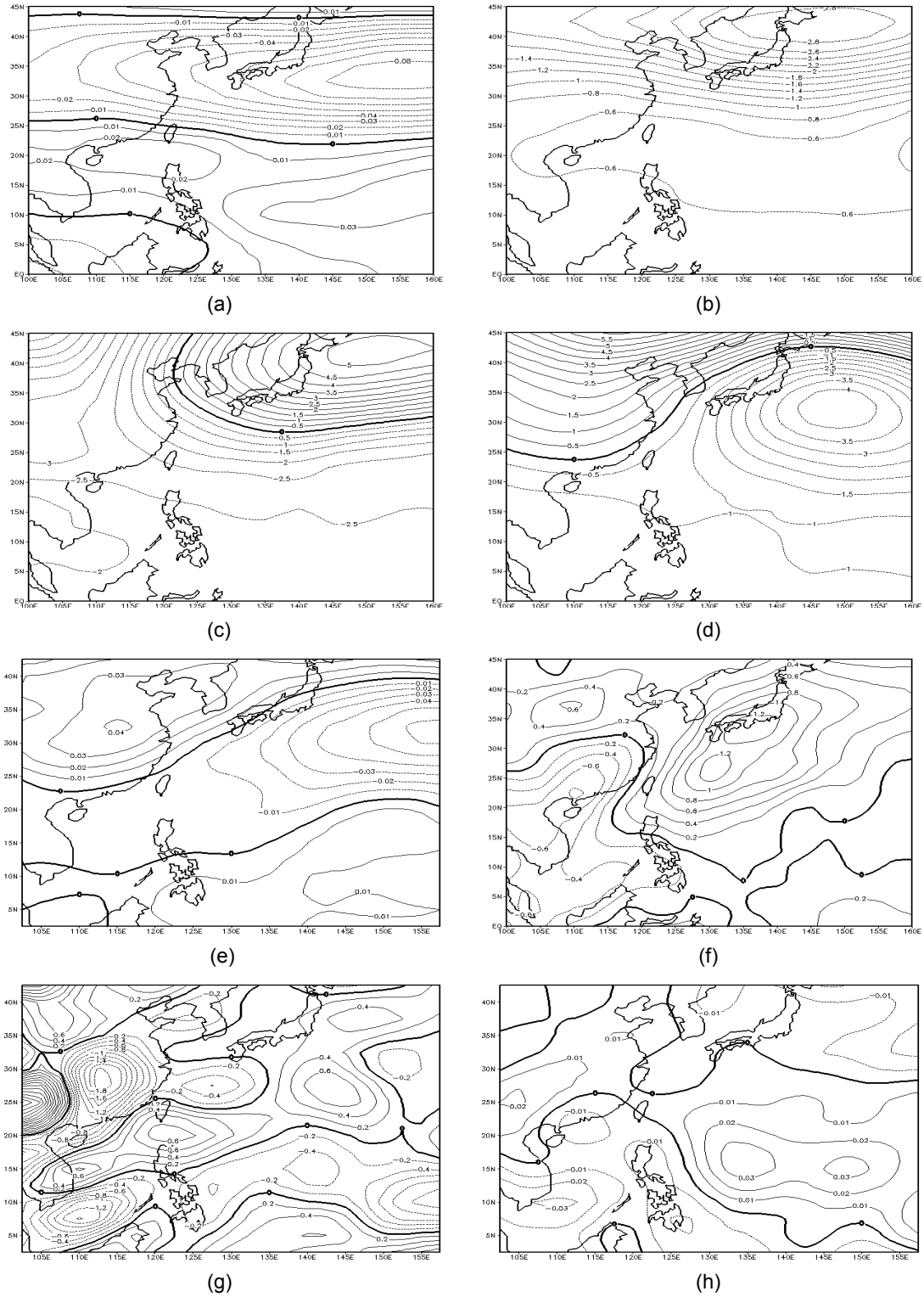

Figure 11 Same as Fig. 9, except for PDO+.

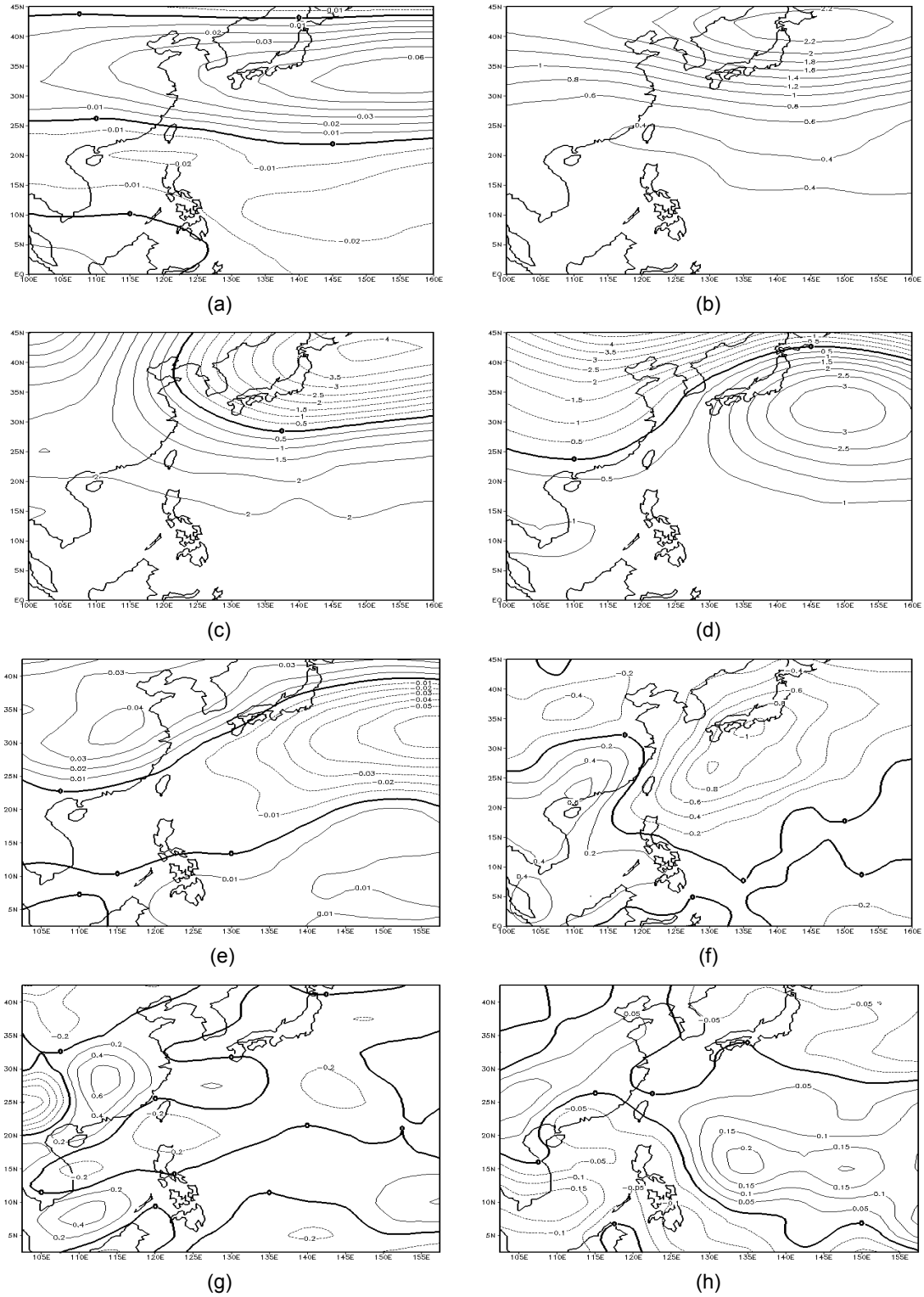

Figure 12 Same as Fig. 9, except for PDO-.